Numerical Simulation on Welding Residual Stress and its Effects on Loading Behavior of Extended Arm Structure

Ang Ji [1], Minggang Chen [2], Liping Zhang [3], Binbin Zhang [2] and Le Gao [1]
[1] XCMG Research Institute Co., Ltd,Xu Zhou, China
[2]XCMG Fire-fighting Safety Equipment Co., Ltd, Xu Zhou, China
[3]State Key Laboratory of Intelligent Manufacturing of Advanced Construction Machinery, Xu Zhou, China

Keywords: Extended arm structure, welding residual stress(WRS), numerical simulation, welding deformation, loading behaviour.

Abstract: In this article, the numerical simulation method was utilized to investigate the welding deformation and residual stress of the extended arm structure. Then the distortion and stress distribution of extended arm structure under loading state were calculated with and without considering the welding residual stress(WRS). The results show that the welding residual stress around weld toe is very high and the maximum Von Mises stress in weld zone is up to 550MPa, which is more than 3 times higher than that of middle area. When welding situation is taken into consideration, the Von Mises stress around the weld area reaches the yield strength of base metal while the Von Mises stress apart from the weld area decreases on account of the offset by WRS. The welding deformation is the main part of the structural deformation in X and Z direction under welding&static situation and the deformation in Y direction is 38.28mm, which is the stack of welding deformation and down warping with static load.

1 INTRODUCTION

Residual stresses are self-equilibrating stresses that are present within a structure when no external forces are applied[1-3]. Typically, kinds of material processing and fabrication techniques create a residual stress in workpiece. One of the most common and high residual stress is caused by conventional welding process near the welding region in metallic structures, where extremely uneven plastic deformation, temperature change and phase transformation in different degree occur[4]. During the serving process, the actual stress is very complicated based on the stack of WRS and working stress, which is bound to have a certain effect on the loading behavior and fracture resistance[5].

Many scholars have studied the WRS and its influence on the bearing capacity of the structure. Li Yanjun et al.[6] analyzed the influence of WRS on the load bearing capacity of the container y-shaped ring joint by using the finite element analysis method. The results showed that the axial tension stress was obviously enlarged by the combined action of WRS and internal pressure and the maximum stress of the Y-ring under loading also enlarged a little. Xiao Qi[7] set the air cylinder as research object and analyzed the influence of WRS on the result of air cylinder structure strength calculation, finding that the existence of WRS could lead to the change of weak link location of structural strength in cylinder body and the bearing capacity decreased obviously.

XuLei[8] investigated the influence of WRS in welding zone of spherical shell on the ultimate bearing strength and come to a conclusion that WRS played little or no role in the ultimate bearing strength which provided certain reference on the post weld stress relief treatment. Takeshi MIYASHITA[9] researched the load-carrying capacity of joint between I shaped girder and thick plate by stress free method and the test results confirmed that the slope of stress distribution in the plate thickness direction increases as the thickness of the plate increases and the residual stress in the thick plate does not affect the load-carrying capacity for the bending of steel girders.

The extended arm is a commonly used welding structure in the field of engineering machinery, and its bearing capacity is directly related to the construction and safety performance of the whole machine[10]. During the static load calculation of the general preliminary structure design, the

designer mainly ensure the safety by expanding the safety factor, and there is no specific analysis on the influence of residual stress on the structure loading behavior. Therefore, based on the extended arm as the research object, the influence of WRS on the loading behavior is analyzed through the finite element simulation method so as to provide certain reference for the design of whole structure and welding process.

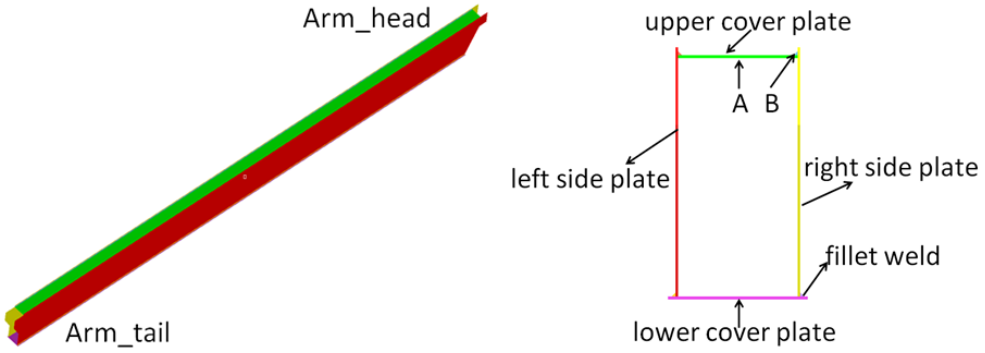

Fig.1 The geometrical model and section form of the extended arm.

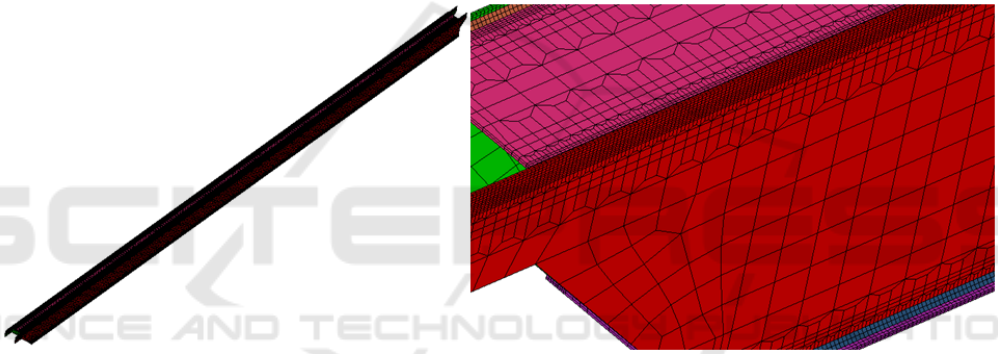

Fig.2 Grid model of extended arm structure.

2 PHYSICAL MODEL OF EXTENDED ARM STRUCTURE

The extended arm structure is set as the research object of welding and structure finite element analysis in this article. The WRS and its influence on loading behavior is the main investigation contents, hence the finite element model only includes the upper and lower cover plate, left and right side plate as well as fillet welds. The geometrical model and section form of the extended arm are shown in Fig.1.

The material used for extended arm is Q550 and the carbon dioxide gas shielded welding method is utilized for four fillet joints with the welding power Fronius TPS5000. There is no groove on the plate and the weld shall be cleaned before welding. The welding process parameters are shown in Table 1.

Table.1 Welding process parameters.

Name	Current I/A	Voltage U/V	Velocity V/(mm·s^{-1})
Value	170~180	19~20	9

3 FINITE ELEMENT ANALYSIS MODEL OF EXTENDED ARM

3.1 Generation of Extended Arm Grid Model

The geometrical model of extended arm is partitioned into solid grid model with 8 nodal hexahedral element[11]. The base mental is divided

into 2~3 layers in order to ensure the accuracy of calculation and the size of grid around weld and HAZ is controlled at 2mm so as to improve the calculation speed, while the size of grid remote from welding zone is 12mm. Two element transitions are adopted in the width direction among the above-mentioned regions to ensure the accuracy of calculation and reduce the number of elements. As shown in Fig.2, the element number of grid model is 344294.

3.2 Material Property Parameters

Q550 is a typical high strength structural steel used in engineering machinery field. It is assumed that the whole model has the same thermal physical property parameters with the change of temperature. The base metal and welding wire are set to have isotropic properties: poisson's ratio is 0.33, mass density is 7870 kg/m3, and the other parameters such as thermal conductivity, specific heat, elastic modulus, thermal expansion coefficient with the temperature change are shown in Fig.3.

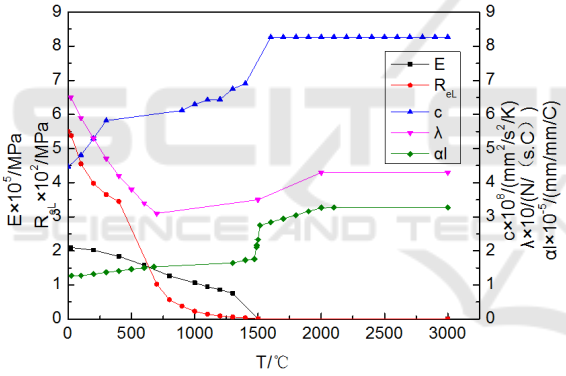

Fig.3 The relationship between heat-force parameters and temperature of Q550.

3.3 Boundary Conditions and Loads

In the process of establishing the welding finite element model, the Goldark double ellipsoid heat source is selected as the boundary condition of the welding heat source[12]. Since there is a temperature difference between the workpiece surface and the surrounding environment during the actual welding process, the Newton's law and boltzmann's law are taken into consideration respectively in the process setting of the convection and radiation dissipation between workpiece and external environment[13].

In the model calculation of welding process, the solid-state phase transformation and work hardening of low carbon steel are ignored for the reason that both of them have little influence on welding residual stress and deformation. The extended arm is in a free state during the welding process, and the mechanical boundary conditions are set to prevent the rigid body displacement of the model.

In the static analysis of the extended arm, the condition that the extended arm is in the horizontal state and the load in the arm head is 2000N is taken into consideration in this paper. As shown in Fig.4, the element of the arm head is connected by RBE2 unit and the load in Y direction is set as 2000N. In actual situation, the main constraint boundary conditions at the end of arm are contact constraints with the follow arms, which is most accurate. However, owing to the influence of WRS on the loading behavior of the extended arm is mainly discussed in this calculation, the other RBE2 rigid connection is added to impose a direct displacement constraints at the end of the extended arm.

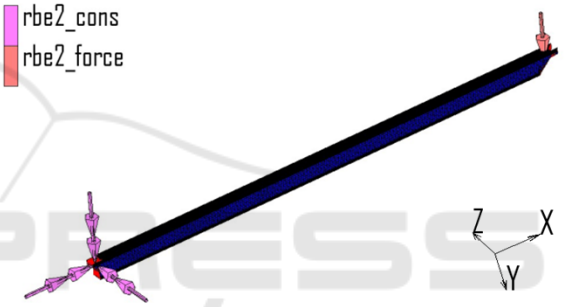

Fig.4 Boundary condition of extended arm static analysis.

4 COMPARISON AND ANALYSIS

4.1 Analysis of Welding Deformation and Residual Stress

Based on the above-mentioned welding boundary conditions, the model is set and the welding load is solved. After the calculation is completed, the welding deformation and welding residual stress of the extended arm are extracted. The welding deformation contours in X, Y and Z direction are shown in Fig.5, from which some results can be achieved that the extended arm is mainly contracted in X direction and the total shrinkage is 6.12mm, while In Y direction, the extended arm is down warped and the downward deflection is 1.15mm. The main reason for above distortion is that the welding seams of the upper cover plate and the lower cover plate are on the different planes and the distance between two weld seams on the upper cover plate is less than that on the lower cover plate. The

deformation of extended arm in Z direction is mainly the contraction deformation along the section direction and the amount is very small. Fig.6 shows the VONMISES stress contour of extended arm structure. It can be seen that the largest equivalent stress occurred in the weld region and the largest equivalent stress is up to 550 MPa which has reached the yield strength of base metal.

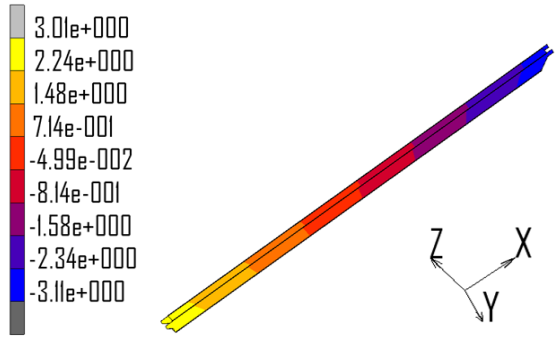

(a) Welding deformation contour in X direction

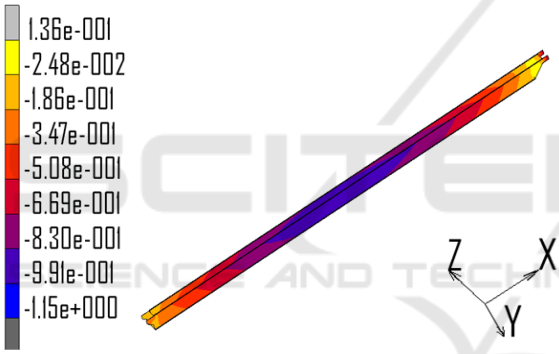

(b) Welding deformation contour in Y direction

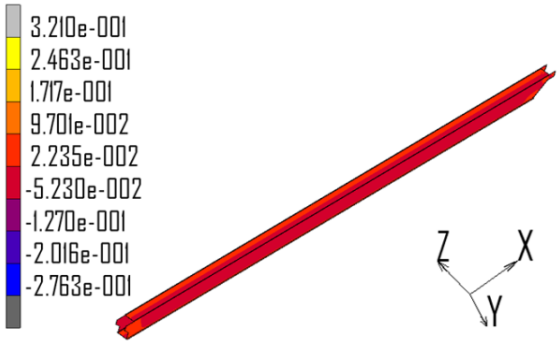

(c) Welding deformation contour in Y direction

Fig.5 Welding deformation contour of extended arm structure.

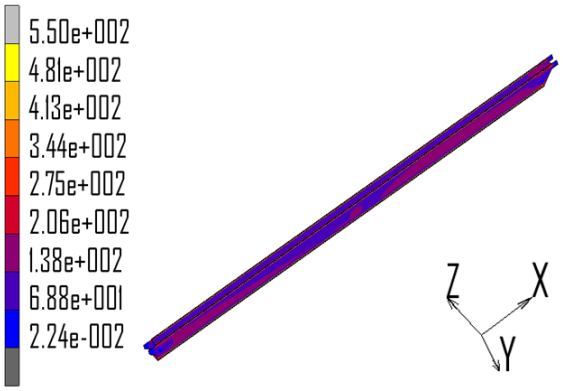

Fig.6 The Von Mises stress contour of extended arm structure.

4.2 Structure Analysis Without Considering the Welding Residual Stress

Based on the above-mentioned static analysis boundary conditions, the model is set and solved. After the calculation is completed, the deformation and working stress of the extended arm are extracted. As the load is applied in the Y direction, the main focus is on the displacement of the extended arm in Y direction. Fig.7 shows the displacement distribution of extended arm in Y direction, as can be seen, the maximum structural deformation of the extended arm occurs in the position of the arm head, and the deformation amount is 36.19mm. The maximum deformation of the upper cover plate in X direction is 0.98mm, while the maximum deformation of the lower cover plate in X is -1.09mm. The deformation of extended arm in Z direction is smaller and negligible since the effect of side load is not considered. Fig. 8 shows the overall Von Mises stress contour of the extended arm structure. As can be seen from the figure that the maximum Mises stress with its value being 114Mpa is located in the restrained position of the extended arm.

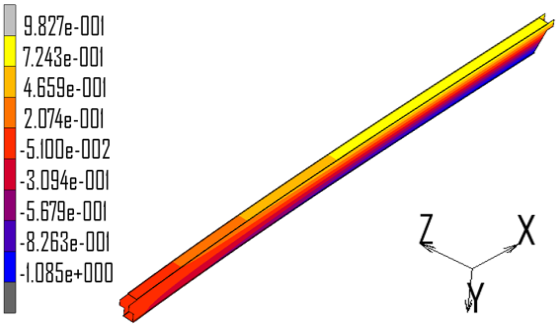

(a) Displacement distribution contour in X direction

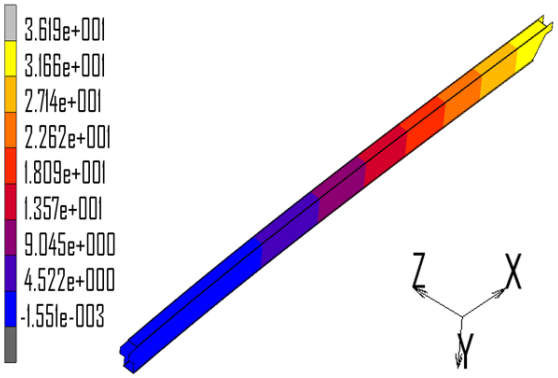

(b) Displacement distribution contour in Y direction

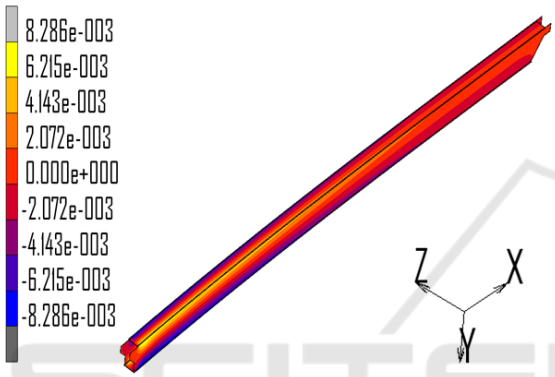

(c) Displacement distribution contour in Z direction

Fig.7 Displacement distribution contour of extended arm structure.

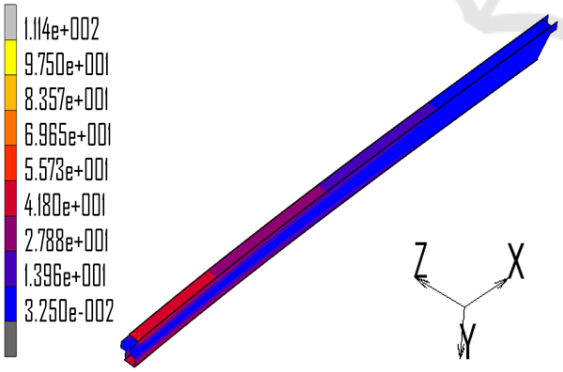

Fig.8 Von Mises stress distribution of extended arm structure.

4.3 Structural Static Analysis Considering the Welding Residual Stress

Based on the above-mentioned welding and static analysis boundary conditions, the model is set and solved. After the calculation is completed, the deformation and working stress of the extended arm are extracted. The displacement distribution contours of extended arm in X, Y and Z direction are shown in Fig.9, from which some results can be achieved that the deformation of the extended arm is still mainly in the Y direction, the largest welding deformation occurs in the position of arm head, and the deformation amount is 38.28mm. Besides, the extended arm is contracted in X direction and the total shrinkage is 6.6mm. Fig.10 shows the Von Mises stress contour of whole extended arm structure. It can be seen that the largest Mises stress occurred in the weld region and the largest equivalent stress is up to 550 MPa which has reached the yield strength of base metal.

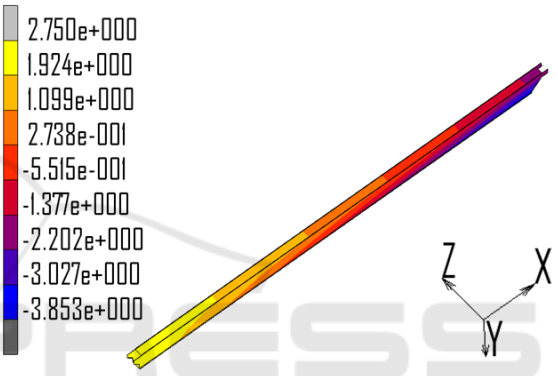

(a) Displacement distribution contour in X direction

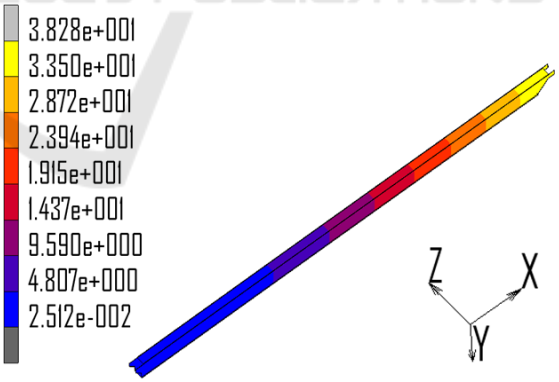

(b) Displacement distribution contour in Y direction

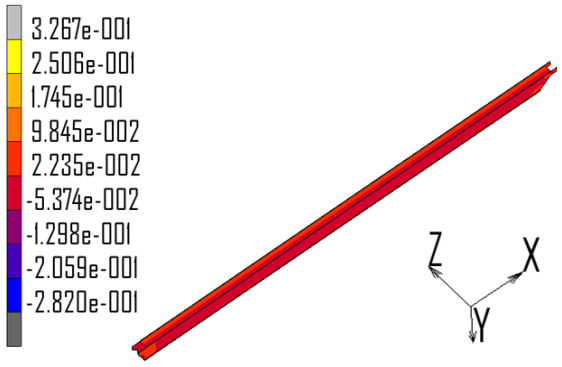

(c) Displacement distribution contour in Z direction

Fig.9 Displacement distribution contour of extended arm structure

Fig.10 Von Mises stress distribution of extended arm structure

4.4 Comparison and Analysis

In order to compare the stress distribution under different conditions(welding, welding&static, static), the stress distribution data along the length direction in position A and B shown in Fig.1 are extracted. The stress distribution is shown in Fig.11.

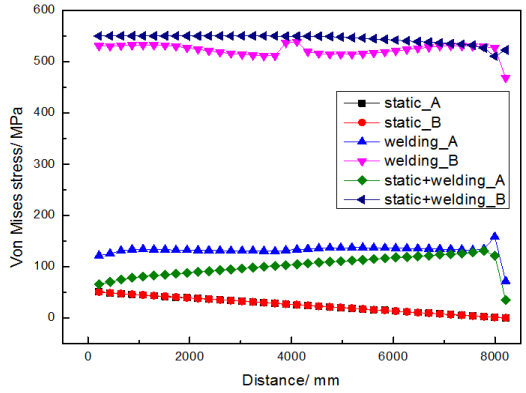

Fig.11 Comparison of Von Mises stress under different conditions.

As can be seen from the diagram, the Von Mises stress in position B is much higher than that in position A and the average Von Mises stress around weld toe is more than 3 times higher than that of middle area. The reason for the high value of stress in position B is that the welding toe is located at the junction of fusion zone and base metal where the gradient of temperature change is large and the plastic deformation is very uneven. The Von Mises stress curves of two positions are basically coincident under static conditions, the main reason for this phenomenon is the bending moment of both positions are almost identical owing to the same distance to the centroid of extended arm structure. With the increase of the length of extended arm, the bending moment caused by the external force decreases gradually, resulting in the decrease of Von Mises stress of position A and position B gradually.

The Von Mises stress in position B is still much higher than that in position A under welding&static conditions, which has little difference from the value in welding condition. The main stress in position B mainly comes from the welding residual stress. In addition, the Von Mises stress in position A is smaller than the WRS in welding condition, the reason for decrease is that the stress in X direction caused by welding as shown in Fig.12 is pressure stress which can be offset by the tensile stress in static condition.

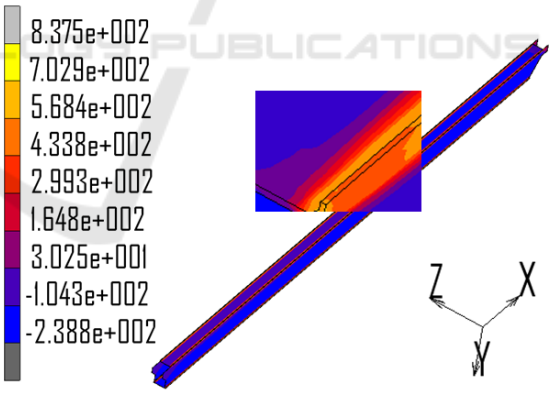

Fig.12 Welding residual stress of extended arm in X direction.

Tab.2 shows the comparison of extended arm deformation in different conditions, from which can we find that the deformation in X direction in welding&static condition mainly results from the welding deformation. The deformation in Z direction in welding&static condition mainly comes from the welding deformation as well. The deformation value in Y direction is 36.19 mm under load in static condition, while the value comes to 38.28 mm in

welding&static condition which mainly results from the stack of welding deformation and downwarping with static load.

Tab.2 Comparison of extended arm deformation in different conditions.

	X_{min}/m	X_{max}/m	Y_{min}/ mm	Y_{max}/m	Z_{min}/ mm	Z_{max}/ mm
Welding	-3.11	3.01	-1.15	0.14	-0.28	0.32
Static	-1.08	0.98	0	36.19	-0.01	0.01
Welding&static	-3.85	2.75	0.03	38.28	-0.28	0.33

5 CONCLUSIONS

(1) The welding deformation and residual stress of the extended arm structure is investigated in the numerical simulation method. The results show that the welding residual stress around weld toe is very high and the maximum Mises stress in weld zone is up to 550MPa, which is more than 3 times higher than that of middle area.

(2) The Von Mises stress around the weld zone in welding&static condition is up to 550 MPa, which is mainly influenced by the welding residual stress, while the stress apart from the weld area decreases on account of the offset by the WRS.

(3) The welding deformation is the main part of the structural deformation in X and Z direction under welding&static condition and the deformation in Y direction is 38.28mm, which is the superposition of welding deformation and downwarping with static load.

REFERENCES

1. Flores-Johnson E A, Muránsky O, Hamelin C J, et al. Numerical analysis of the effect of weld-induced residual stress and plastic damage on the ballistic performance of welded steel plate[J]. Computational Materials Science, 2012, 58:131-139.
2. Nikkarila J P, Manninen M. Introduction to the characterization of residual stress by neutron diffraction /[M]. Taylor & Francis, 2005.
3. Lammi C J, Lados D A. Effects of residual stresses on fatigue crack growth behavior of structural materials: Analytical corrections[J]. International Journal of Fatigue, 2011, 33(7):858-867.
4. Cheng Xiaoyu, Wang Xiaomei. The essence and adjustment of residual stress[J]. Total corrosion control, 2009, 23(7):33-35.
5. GaoZhanyuan, GuoYanlin.Analysis on Influence of welding residual stress on ultimate bearing capacity of Y-joints[J]. Journal of architectual science and engineering, 2016, 33(6):73-80.
6. Li Yanjun, Wu Aiping, Liu Debo, et al. Numerical simulation on Y-ring welding residual stress and its effects on loading behavior of propellant tank[J].Transactions of nonferrous metals society of china, 2017, 27(4):701-707.
7. Xiao Qi. Study on numerical method of strength analysis based on coupling method of welding residual stress and service load[D]. Beijing Jiaotong University, 2014.
8. Xu Lei, Huang Xiaoping, Wang Fang. Effect of welding residual stress on the ultimate strength of spherical pressure hull [J]. Journal of ship mechanics, 2017, 21(7):864-872.
9. Miyashita T, Inaba N, Hirayama S, et al. Measurement method for welding residual stress in steel I-shaped girder with thick flange and its influence on load carrying capacity for bending[J]. Structural Engineering, 2015, 3:191-208.
10. Liu Min. Structure analysis and optimization of autocrane [D]. Chang an university, 2014.
11. Wang Changli. Numerical simulation of welding temperature distribution and stress variation [D].Shenyang University of Technology,2005.
12. John Goldak，AdityaChakravarti，Malcolm Bibby．A new finite element model for welding heat sources[J]．Metallurgical Transactions B，1984(15)：299-305．
13. Deng D. Theoretical prediction of welding distortion in thin curved structure during assembly considering gap and misalignment [D]. Doctoral Thesis, Osaka University, 2002.